A numerical simulation of a classical dipolar spin system and a demonstration with magnetic compasses

Takeshi Nishimatsu[1,2,3], Umesh V. Waghmare[4], Yoshiyuki Kawazoe[1], Benjamin Burton[5], Kazutaka Nagao[6], and Yoshihiko Saito[7]

We report a simple, safe and stimulating pedagogical demonstration with magnetic compasses that facilitates intuitive understanding of dipolar interactions and their consequences in magnetic materials. We determine and discuss special states of classical dipolar spin systems corresponding to minima, maxima, and saddle-points of their energy surface. While our results for finite systems readily show how one can expect interesting effects in nano-scale ferroelectric and ferromagnetic materials, our analysis of macroscopic systems reveals low energy states of magnetic ordering and the transition states on the paths of switching between them. A computer program developed for numerical analysis of these model systems, based on the concepts of force constant matrix and an iterative energy-minimization scheme, can be readily used along with a lab-demonstration with magnetic compasses.

I. INTRODUCTION

Long-range dipole-dipole interaction plays important roles in ferromagnets and ferroelectrics, especially in the formation of domain structures[1]. For example, in *finite* ferroelectric systems, surface charges associated with uniform spontaneous polarization $\boldsymbol{P}$ cause depolarization field which has an opposite direction to $\boldsymbol{P}$, due to the inherently long-range interaction. In general, for reducing the overall energy in the presence of depolarization field, finite systems exhibit domain structures and stabilize. But the dipole-dipole interaction, due to its long-range and strongly anisotropic nature, is not an easy problem for beginners in physics and material science.

It is also known that the stable states of dipolar spin systems are sensitive to periodicity, dimensionality, boundary conditions (finite or infinite), size, aspect ratio[2], symmetry, and defects. Recent developments in nanotechnology introduce a new paradigm for ferromagnetic and ferroelectric finite-size particles and wires: e.g. an x-ray photo-lithography[3], a mask technique with molecular bean epitaxy (MBE)[4], and a solution based method[5,6]. The role of dipole-dipole interaction has become more important than ever in such dipolar nano-systems.

Microscopic dipolar spin systems have been studied in crystals and crystalline surfaces[7], and in interfaces. Recently, however, Wang *et al.* used a lithographic method[8] to synthesize a two-dimensional *nanoscale* frustrated dipole system of 80,000 elongated permalloy ($Ni_{0.81}Fe_{0.19}$) islands on a native-oxide covered silicon surface.

Here, we provide a *macroscopic* model for classical dipolar spin system: an array of magnetic-compasses, in which compasses (classical spins) interact via magnetic dipole-dipole interaction. This system is safe, simple, inexpensive, rearrangeable, and can be easily manipulated with hands and/or magnets.

In the following section (Sec. II), we introduce setup of laboratory demonstration with magnetic compasses and describe some interesting results obtained with it. In Section III, We discuss briefly the methods used in computational analysis and its results for ground and other special states of various cases of dipolar spin systems. We also point out the differences between infinite and finite dipolar systems. Finally, we summarize in Section IV.

II. MAGNETIC COMPASS DEMONSTRATION

If one puts two magnetic compasses on a table, well separated from each other, both point north as pictured in Fig. 1(a); i.e. earth's magnetic field (24–66 μT) dominates the dipole-dipole interaction. As one brings them closer together, however the dipole-dipole interaction takes over below a certain distance. Compass needles, then, align along the line between them, i.e. $<\mathrm{S\,N}><\mathrm{S\,N}>$ in Fig. 1(b). As in Fig. 1(c), if one puts three, four, or more compasses in a row, one also finds that they align according to $<\mathrm{S\,N}><\mathrm{S\,N}><\mathrm{S\,N}>\cdots$. Now, if we arrange the compasses in a square array on a board and give a jiggling to the board, the compass needles relax into the states pictured in Fig. 2. As discussed in section III, such systems have minimum, maximum, and saddle-point states. Figs. 2(a) and (b) are minimum states.

[1] Institute for Materials Research (IMR), Tohoku University, Sendai 980-8577, Japan
[2] Department of Physics and Astronomy, Rutgers University, 136 Frelinghuysen Road, Piscataway, NJ 08544-8019
[3] Japan Society for the Promotion of Science (JSPS) Postdoctoral Fellow for Research Abroad
[4] Theoretical Sciences Unit, Jawaharlal Nehru Centre for Advanced Scientific Research (JNCASR), Jakkur, Bangalore, 560 064, India
[5] National Institute of Standards and Technology (NIST), 100 Bureau Drive STOP 8520, Gaithersburg, MD 20899-8520
[6] Research Institute of Electrical Communication (RIEC), Tohoku University, Sendai 980-8577, Japan
[7] Osaka Science Museum, 4-2-1 Nakanoshima, Kita-ku, Osaka 530-0005, Japan

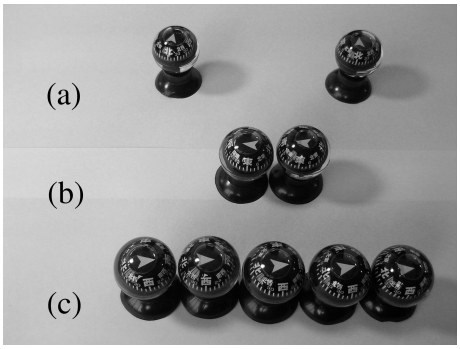

FIG. 1: (a) Two car-windshield magnetic compasses on a table, sufficiently far apart they both point north. (b) sufficiently close together, the dipole-dipole interaction dominates. (c) Five compasses in a row.

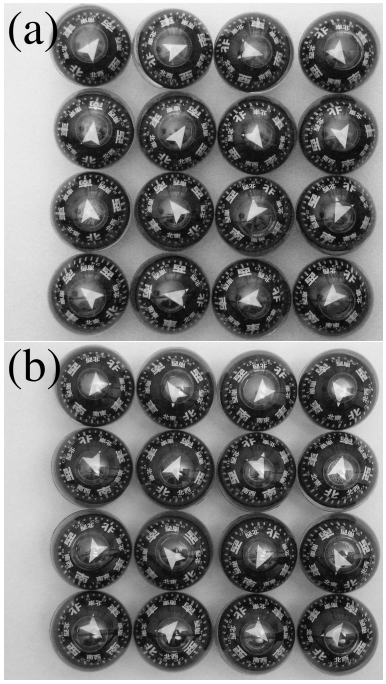

FIG. 2: Observed stable states in the 4×4 square magnetic-compass array. In section III, it will be explained that (a) and (b) are minimum states and (b) is the ground state.

One of the authors, YS, invented this demonstration[9] and displayed a triangular array with about 1000 magnetic compasses in the Osaka Science Museum as depicted in Fig 3(a). The domain structure clearly visible (Fig 3(b)) in this finite and symmetric triangular array has been attracting both children and adults, and stimulating more questions pertaining to the nature of magnetism in crystals.[10]

These experiments are easily performed when one uses magnetic compasses that are designed for use on automobile windshields, as shown in Figs. 1, 2, and 3. Each compass has a transparent 28 mm diameter bubble-like plastic container filled with oil, a suction cup for attaching it to a windshield, and a ferrite permanent magnet arrow that floats freely in the oil. Dimensions of the ferrite magnet are $8 \times 6 \times 3$ mm. The 8×3 mm arrow sides are magnetic poles with surface magnetic fields of ≈ 50 mT, that decay to 1.5 mT at the surface of the plastic container. For compasses of this strength, the influence of earth's magnetic field on them can be neglected in comparison with that from the interaction between two compasses, if they are placed within 50–60 mm of each other. For compasses arranged on a square array such that the nearest neighbor compasses touch each other, dipole-dipole interactions dominate over the influence of earth's magnetic field for the first three nearest neighbor compasses.

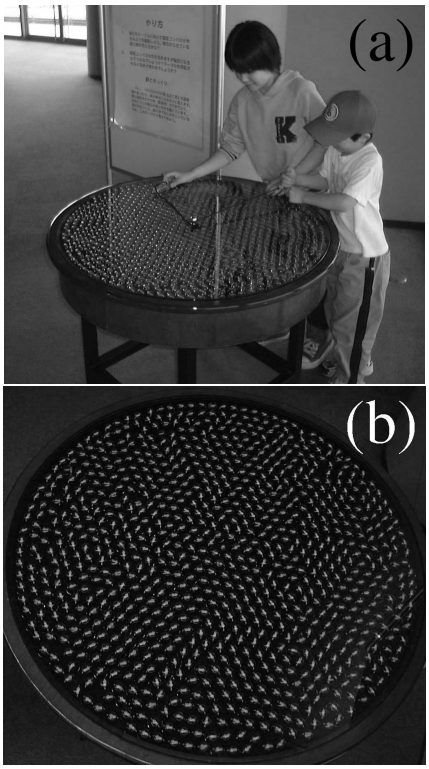

FIG. 3: (a) A triangular array of about 1000 magnetic compasses, on a rotating table top, that is on display in the Osaka Science Museum. (b) Magnetic domains are visible. Observers can make sure that the effects of earth's magnetic field is negligible by rotating the table on which compasses are placed. Domain structures do not change when the table is rotated.

III. COMPUTATIONAL ANALYSIS

A. Force constant matrix

Consider a 2-dimensional finite system of N dipoles. The dipoles are placed at coordinates $\boldsymbol{r}_I = (x_I, y_I)$, $I = 1, \cdots, N$, their momenta are $\boldsymbol{\mu}_I = (\mu_{Ix}, \mu_{Iy})$, and their interactions are exclusively dipole-dipole in charac-

ter. The total interaction energy V is

$$V(\{\boldsymbol{\mu}_I\}) = \frac{1}{2}\sum_{I\alpha}\sum_{J\beta}\mu_{I\alpha}\Phi_{I\alpha,J\beta}\,\mu_{J\beta}\ , \tag{1}$$

where α and β are independent orthogonal directions (x and y), and $\Phi_{I\alpha,J\beta}$ is the force constant matrix

$$\Phi_{I\alpha,J\beta} = -\frac{\partial}{\partial r_{I\alpha}}\frac{\partial}{\partial r_{J\beta}}\frac{1}{|\boldsymbol{r}_I - \boldsymbol{r}_J|} = \frac{\delta_{\alpha\beta} - 3(\widehat{\boldsymbol{r}_{IJ}})_\alpha(\widehat{\boldsymbol{r}_{IJ}})_\beta}{|\boldsymbol{r}_{IJ}|^3}\ , \tag{2}$$

where $\boldsymbol{r}_{IJ} = \boldsymbol{r}_I - \boldsymbol{r}_J$, a hat indicates a vector of unit magnitude, e.g. $\widehat{\boldsymbol{r}} = \boldsymbol{r}/|\boldsymbol{r}|$, and $\Phi_{I\alpha,J\beta} = 0$ for $I = J$. We fix the amplitude of each moment $\boldsymbol{\mu}_I$ to unity,

$$\sum_\alpha \mu_{I\alpha}^2 = \mu_{Ix}^2 + \mu_{Iy}^2 = 1\ , \tag{3}$$

to simulate the magnetic-compass system. For finding extrema (minima, maxima, and saddle-points) of the total interaction energy (1), subject to the constraint (3), we use an iterative minimization technique: First, only once at the beginning, we prepare the force constant matrix as in (2). From a spin configuration $\mu_{I\alpha(k)}$ of the k-th iteration, we evaluate the force exerted on each dipole, $-\sum_{J\beta}\Phi_{I\alpha,J\beta}\,\mu_{J\beta(k)}$, then, we update from $\mu_{I\alpha(k)}$ to $\mu_{I\alpha(k+1)}$:

$$\mu_{I\alpha(k+1)}{}' = \mu_{I\alpha(k)} - \gamma\sum_{J\beta}\Phi_{I\alpha,J\beta}\,\mu_{J\beta(k)}\ , \tag{4}$$

with normalization to satisfy the fixed-amplitude restriction (3),

$$\boldsymbol{\mu}_{I(k+1)} = \frac{\boldsymbol{\mu}_{I(k+1)}{}'}{|\boldsymbol{\mu}_{I(k+1)}{}'|}\ . \tag{5}$$

In Eq. (4), γ is the adjustable dumping factor for steady minimization. Larger positive γ may achieve faster convergence to the minima but may possibly fall into an oscillation in the updating scheme. On the other hand, if γ is set to a negative value, the scheme will converge to a maximum energy state. The initial guess of spin configuration $\mu_{I\alpha(1)}$ determines which specific special (minimum, maximum or saddle-point) state the scheme will converge to.

The total interaction energy V is also expressed in rotational angle θ_I of each dipole as

$$V(\{\theta_I\}) = \frac{1}{2}\sum_{I\neq J}\frac{\cos(\theta_J - \theta_I) - 3\cos(\theta_J - \phi_{IJ})\cos(\phi_{IJ} - \theta_I)}{|\boldsymbol{r}_{IJ}|^3}\ , \tag{6}$$

where ϕ_{IJ} is the rotational angle of $\boldsymbol{r}_{IJ}$, i.e. $\tan\phi_{IJ} = y_{IJ}/x_{IJ}$. Because the first θ_I derivertives of Eq. (6) are zero for all I in the neighborhood of extremum $V^0 = V(\{\theta_I^0\})$, the total interaction energy can be expressed with deviation angles $\delta\theta_I$ of each dipole as

$$V = V^0 + \sum_I\sum_J \left.\frac{\partial^2 V}{\partial\theta_I\partial\theta_J}\right|_{\theta_I=\theta_I^0,\theta_J=\theta_J^0}\delta\theta_I\delta\theta_J, \tag{7}$$

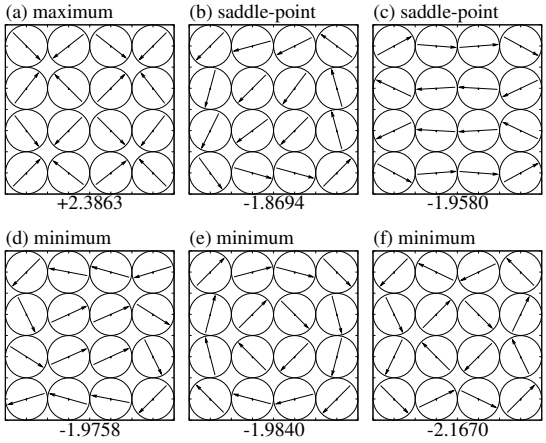

FIG. 4: Maximum state (a), saddle-point states (b) and (c), and minimum states (d)–(f) for the 4×4 square array. (f) is the ground state. Below each panel, averaged interaction energy per dipole $V/16$ is indicated. In the idealized system, the dipoles are "points" at each center of circle. Here, we emphasize the directions of dipoles and their packings with arrows and circles.

where for $I \neq J$,

$$\frac{\partial^2 V}{\partial\theta_I\partial\theta_J} = \frac{\cos(\theta_J - \theta_I) + 3\sin(\theta_J - \phi)\sin(\phi - \theta_I)}{|\boldsymbol{r}_{IJ}|^3}\ , \tag{8}$$

and for $I = J$,

$$\frac{\partial^2 V}{\partial\theta_I^2} = \sum_{J\neq I}\frac{-\cos(\theta_J - \theta_I) + 3\cos(\theta_J - \phi)\cos(\phi - \theta_I)}{|\boldsymbol{r}_{IJ}|^3}\ . \tag{9}$$

Using this θ_I expression of the total interaction energy, we can classify extrema into minimum, maximum, and saddle-point states: At the "minimum state", all the eigenvalues of the $N \times N$ matrix $\left.\frac{\partial^2 V}{\partial\theta_I\partial\theta_J}\right|_{\theta_I=\theta_I^0,\theta_J=\theta_I^0}$ are positive. At the "maximum state" all the eigenvalues are negative. At the "saddle-point state" some of eigenvalues are positive and others are negative. We also define the "ground state" as the lowest-energy minimum state. In following two subsections, using the minimization scheme (4) and (5), we search ground states of some square and triangular dipole arrays which have high symmetries.

B. Square array of dipoles

In Fig. 4, we show the calculated maximum, saddle-point, and minimum states for the 4×4 square array. It is very interesting that the state shown by Fig. 4(c) is a saddle-point state. On the demonstration with the magnetic compasses, the state as Fig. 4(c) behaves like a stable state. It may be thought that this phenomenon shows a reasonable state as follows. When the set of 4×4 dipoles is divided into by half of the top and bottom, the structure of Fig. 4(c) is made of two clusters of

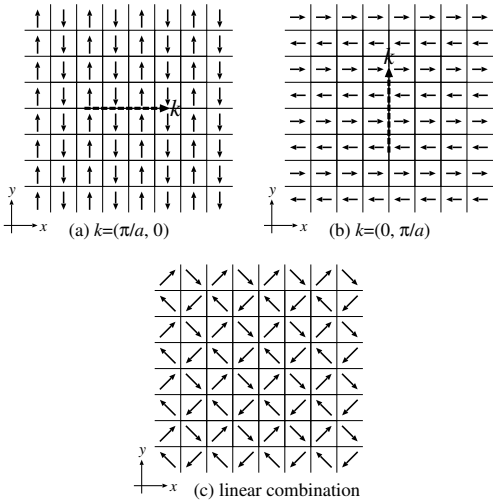

FIG. 5: (a) Antiferromagnetic ground-state of the infinite periodic dipole square lattice which has wave vector $\boldsymbol{k} = (\pi/a, 0)$, i.e. $\boldsymbol{\mu}(\boldsymbol{r}_I) = (0, 1)\exp[i\frac{\pi}{a}x_I]$, where a is the distance between nearest neighbor dipoles. $\boldsymbol{\mu}(\boldsymbol{r}_I)$ are illustrated with small arrows at each site. The direction of the wave vector $\boldsymbol{k}$ is indicated with a dashed arrow. (b) Degenerate antiferromagnetic ground-state which has wave vector $\boldsymbol{k} = (0, \pi/a)$, i.e. $\boldsymbol{\mu}(\boldsymbol{r}_I) = (-1, 0)\exp[i\frac{\pi}{a}y_I]$. (c) Canted antiferromagnetic structure which is a linear combination of (a) and (b), i.e. $\boldsymbol{\mu}(\boldsymbol{r}_I) = (0, 1/\sqrt{2})\exp[i\frac{\pi}{a}x_I] + (-1/\sqrt{2}, 0)\exp[i\frac{\pi}{a}y_I]$.

2×4 dipoles, which show the same type on the ground state each other. If these two clusters got closer to from far away each other and the state shown by Fig. 4(c), it would be easily imagined that the structure of Fig. 4(c) is stable with the line symmetry. It, however, is impossible that the magnets of each compass put precisely like Fig. 4(c), because an error of around 10 percentage of the size occurs in structure of each compass. So, the two clusters on the demonstration with the magnetic compasses are stable. If the magnets of each compass put precisely as Fig. 4(c), the line symmetry would brake and they would fall into the structure of Fig. 4(d). It is interesting that the above-mentioned consideration on the saddle-point state shown by Fig. 4(c) and the minimum point shown by Fig. 4(d) resembles the spontaneously broken symmetry on Higgs field in elementary particle physics and creation of the universe in cosmology.

It is surprising that even this high-symmetry 4×4 square array exhibits three kinds of minimum states.

It is known that the ground-state of the *infinite* periodic square lattice of dipoles forms a continuously degenerate manifold of antiferromagnetic states[11], which is a linear combination of two independent spin configurations as illustrated in Fig. 5 (In this report, we use the word "array" for finite systems and "lattice" for infinite periodic systems.). The interaction energy per dipole for the infinite periodic square lattice is -2.5495 (We express the interaction energy in units of μ^2/a^3 the dipole moment squared divided by the nearest neighbor distance cubed.).[7] The averaged interaction energy per

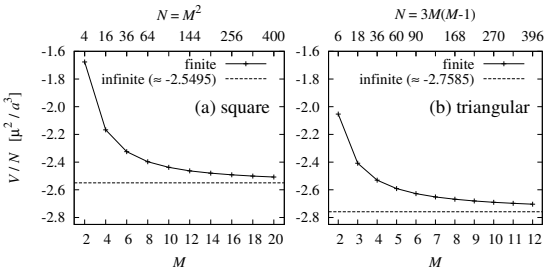

FIG. 6: Ground-state averaged interaction energy per dipole V/N for: (a) $M \times M = N$ finite square arrays; (b) finite triangular arrays with M dipoles on a side and a total of $N = 3M(M-1)$ dipoles. The interaction energy per dipole in the ground-state for the infinite square and triangular lattice system is plotted as dashed holizontal asymptote lines.

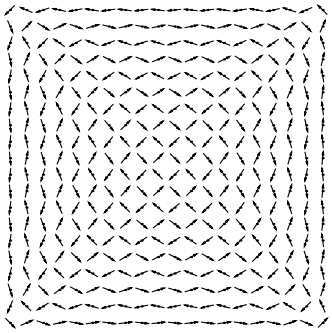

FIG. 7: Calculated ground-state of the $N = 20 \times 20 = 400$ dipole square array.

dipole V/N for the $M \times M = N$ finite dipole square array approaches to -2.5495 as M increases, as illustrated in Fig. 6(a). Figure 7 shows the 20×20 square array, in which the spin configuration in central region array approaches the canted antiferromagnetic structure of the infinite system (Fig. 5(c)). Exactly the same structure as in Fig. 7 is achieved in the 20×20 magnetic compass square array, but some by-hand one-by-one alignments and a jiggling of the board on which compasses are placed are required to reach the ground-state configuration. It seems that friction between the plastic container and the arrow of the compasses preventing the system from falling into its ground state. Compasses with greater accuracy and stronger magnets may reach the ground state more easily.

C. Triangular array of dipoles

We also calculated ground-states for the two different types of finite triangular arrays shown in Fig. 8. Both exhibit six-fold symmetry on their outer edges, but in Fig. 8(a) 6-fold symmetry is broken by the central dipole, while in Fig. 8(b) full six-fold symmetry is maintained. The latter has a defect (a missing dipole) at the centre.

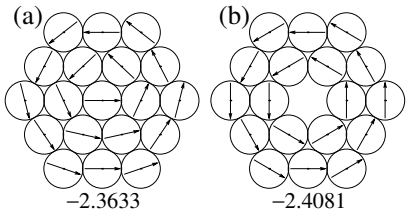

FIG. 8: Ground states of finite triangular arrays with (a) $N = 19$ and (b) $N = 18$ dipoles. The averaged interaction energy per dipole V/N are -2.3633 and -2.4081, respectively.

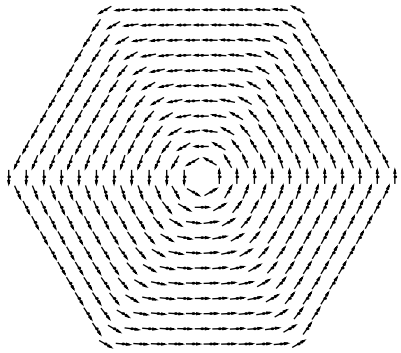

FIG. 9: Calculated ground-state of the $N = 396$ triangular array. Six ferromagnetic domains separated by domain walls are evident.

This demonstrates how sensitive ground-states of finite dipolar systems are to their symmetries, defects and size. This has direct implications to nano-scale electric dipolar systems, for example ferroelectrics.

The ground-state of an infinite periodic triangular lattice of dipoles is also continuously degenerated but *ferromagnetic*.[7] In finite triangular arrays, the continuous degeneracy breaks down, and domains form to reduce the depolarization field as depicted in Fig. 3(b), Fig. 8 or more clearly in Fig. 9. The interaction energy per dipole in the infinite triangular lattice is -2.7585.[7] We evaluate the averaged interaction energy per dipole V/N in the ground-states of finite triangular arrays, e.g. Fig. 8(b) and Fig. 9, in which there are: M dipoles on a side; a total of $N = 3M(M-1)$ dipoles per array; and 6-fold symmetry because they do not have central dipoles. Asymptotic approach of the averaged interaction energy, to that of the infinite system, is shown in Fig. 6(b). Again, a spin configuration that is identical to that in Fig. 9 can be achieved in the magnetic-compass array *with* one-by-one manipulation and a jiggling of the board on which compasses are placed; analogous to simulated annealing.

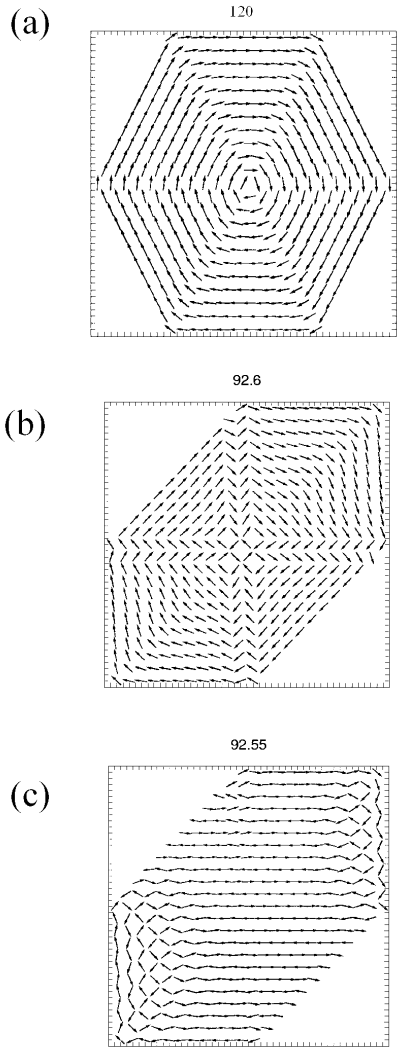

FIG. 10: On a numerical simulation, a crystal structure of the 397 dipoles on a hexagon boundary condition is transformed from the triangle lattice arrangement (a) to the rectangle one by the quasi-static process. Though antiferromagnetism is not observed by 92.6° (b), a phase transition is observed at 92.55° (c).

D. Phase transition between ferromagnetism and antiferromagnetism

We show calculated phase transitions between ferromagnetism and antiferromagnetism. Figure 10 shows the phase transitions transformed from triangle array to the square array of the 397 dipoles on the case of a hexagon boundary condition.

Figure 11 is the case of a diamond boundary condition. Domains of antiferromagnetism grow up from a energetically unstable place, from the center toward the top left side and the lower right one.

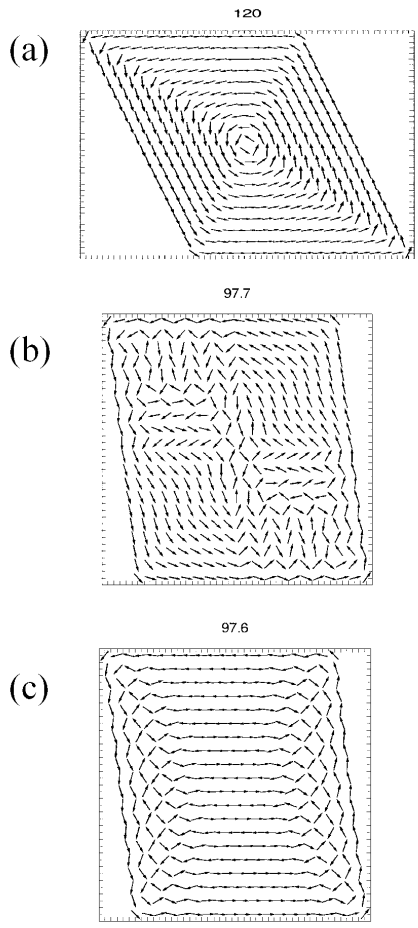

FIG. 11: On a numerical simulation, a crystal structure of the 20×20 dipoles is transformed from the triangle lattice arrangement (a) to the rectangle one by the quasi-static process. Domains of antiferromagnetism grow up toward the top left side and the lower right one from the center by 97.7° (b). A phase transition is observed at 97.6° in the top right side and the lower left one (C).

The angles at which the phase transition occurs depend on the boundary condition. The angles are 97.7° on the case of a diamond boundary condition and 92.55° on the case of a hexagon boundary condition.

Phenomena like these phase transitions can be observed by the demonstration with tha magnetic compasses.[9] [10]

IV. SUMMARY

We introduced an attractive demonstration that uses magnetic compasses to facilitate intuitive understanding of dipolar spin systems. Even with a few dozen cheap magnetic compasses, safe and fascinating experiments can be performed. Maximum, minimum and saddle-point states of finite classical dipole arrays are analyzed by using the force constant matrix and an iterative energy-minimization scheme. This is a good pedagogical tool for teaching how the dipole-dipole interactions influence the structure of special states of dipolar systems.

Acknowledgment

We thank International Frontier Center for Advanced Materials (IFCAM) of IMR who supported UVW to visit to Sendai and authors' collaborative study in ferroelectrics. We would like to extend our gratitude to Professor Gyo Takeda (Emeritus Professor of University of Tokyo and Tohoku University) and Professor Noboru Takigawa (Department of Physics, Tohoku University) who showed TN the demonstration with magnetic compasses invented by YS. We also extend our gratitude to Professor Takayuki Hamaguchi (Nada Junior and Senior High School) who gave suggestive photos and comments of the compass arrays to the authors. We also wish to thank an anonymous referee for a careful reading of our manuscript and a useful comment.

A part of this work was supported by a Grant-in-Aid for Encouragement of Scientists, 2006, No.18912015, from Japan Society for the Promotion of Science.

[1] C. Kittel, *Introduction to Solid State Physics* (Wiley, New York, 2004), 8th ed, Chap. 12 and 16.
[2] P. Politi, M. G. Pini, and R. L. Stamps, Phys. Rev. B **73**, 020405 (2006).
[3] M. Hehn, K. Ounadjela, J. P. Bucher, F. Rousseaux, D. Decanini, B. Bartenlian, and C. Chappert, Science **272**, 1782 (1996).
[4] C. Stamm, F. Marty, A. Vaterlaus, V. Weich, S. Egger, U. Maier, U. Ramsperger, H. Fuhrmann, and D. Pescia, Science **282**, 449 (1998).
[5] J. J. Urban, W. S. Yun, Q. Gu, and H. Park, J. Am. Chem. Soc. **124**, 1186 (2002).
[6] W. S. Yun, J. J. Urban, Q. Gu, and H. Park, Nano Lett. **2**, 447 (2002).
[7] V. M. Rozenbaum, V. M. Ogenko, and A. A. Chuĭko, Sov. Phys. Usp. **34**, 883 (1991).
[8] R. F. Wang, C. Nisoli, R. S. Freitas, J. Li, W. McConville, B. J. Cooley, M. S. Lund, N. Samarth, C. Leighton, V. H. Crespi, et al., Nature **439**, 303 (2006).
[9] Y. Saito and K. Yasue, Frontier Perspectives **10**, 28 (2001).
[10] Y. Saito, Butsuri Kyouiku (Physics Education) **53**, 103 (2005), [in Japanese].
[11] K. De'Bell, A. B. MacIsaac, I. N. Booth, and J. P. Whitehead, Phys. Rev. B **55**, 15108 (1997).